ChemPubSoc Europe

DOI: 10.1002/slct.201801051

Chemistry SELECT Full Papers

Sustainable Chemistry

Etherification of Hydroxymethylfurfural with Preyssler Heteropolyacids Immobilized on Magnetic Composites

Oscar H. Pardo Cuervo,[a] Hugo A. Rojas,[a] Lucas A. Santos,[b] Teodorico C. Ramalho,[b] Gustavo P. Romanelli,[c] and José J. Martínez*[a]

A thermodynamic study about the stability of intermediates in the reaction of 5-hydroxymethylfurfural (HMF) over Preyssler heteropolyacids (HPA-Preyssler) was performed to explain the self-etherification or oxidation of HMF. Although the product of etherification forms in higher proportion when a heteropolyacid is used, other oxidation products are also observed. The availability of HPA-Preyssler protons is essential to conduct the self-etherification; however, this is not favored when the heteropolyacid is immobilized on metallic oxides and besides, the reusability of the supported heteropolyacid is low. In this study, magnetic composites were used to incorporate the HPA-Preyssler to prevent the formation of by-products and to facilitate the separation from the reaction medium. The results of catalytic tests and acidity analysis demonstrated a better proton availability, and the recovery of glutaraldehyde of the heteropolyacid decreases the leaching of immobilized HPA-Preyssler when the composite is reused. The reaction was optimized obtaining a maximum yield to OBMF near 70% in 5 h.

Introduction

5-Hydroxymethylfurfural (HMF) is considered as a renewable platform molecule with the potential to be modified to biofuels and specific molecules in the pharmaceutical industry.[1] One of these compounds is 5,5′(oxibis-(methylene))-bis-2-furfural (OBMF), which is produced from the etherification of two molecules of HMF. OBMF can be used as a monomer for the preparation of some imine-based polymers with high thermal and electrical conductivity,[2] and it can also be used for the synthesis of heterocyclic ligands for hepatitis antiviral precursors.[3]

The best known routes for OBMF synthesis are the etherification reaction of two HMF molecules catalyzed by homogeneous organic acids such as *p*-toluenesulfonic acid and organic solvents such as toluene[4] and by the Williamson reaction between HMF and 5-chloromethyl-2-furfural in an excess of base.[3] Amberlyst-15 has been identified to be a highly active and selective catalyst for the etherification of 5-methylfurfuryl alcohol, 2,5-bis(hydroxymethyl)furan and HMF by C1-C4 alcohols.[5] Likewise, a Brönsted acid heterogenization strategy has been used for etherification reactions, e.g., Fang et al. immobilized the Aquivion® PFSA superacid resin in a silica network via the one-pot template-free sol-gel method to direct the etherification of glycerol with *n*-butanol.[6] Specifically, in the case of OBMF, a number of acidic solids, including mesoporous aluminosilicates,[7] graphene oxide,[8] Amberlyst-15,[9] tin supported on montmorillonite,[10] have been tested in the last 7 years, with excellent yields (50-99%). However, in some cases the reaction conditions are strong (high temperatures and prolonged times).

Recently, our research group reported the synthesis of OBMF by the etherification of 5-HMF under mild reaction conditions using HPA-Preyssler. The etherification of 5-HMF was favored by the higher Brönsted acidity, and the production of OBMF was optimized using bulk HPA-Preyssler, obtaining a selectivity of 95% with 85% of conversion of 5-HMF at 5 h and 343 K. However, Preyssler heteropolyacids present a low surface area and for this reason are generally deposited on different supports, but the interaction between the support and the heteropolyacid decreases the acidity and consequently, the conversion.[11] The lowest proton mobility when the HPA-Preyssler is supported depends on the negative charge distribution in the heteropolyanion oxygens and the electrostatic interaction of the HPA-Preyssler with -OH surface groups of the support, thus a convenient method is the use of composites that can immobilize the heteropolyacid. But by this methodology, to recover the catalyst it is necessary to filter it before each reuse, which could result in the loss of catalyst particles and product contamination.

The HPAs were immobilized on silica material that had been modified with organosiloxanes, e.g., (3-aminopropyl) trimethoxysilane (APTMS) and (3-aminopropyl) triethoxysilane (APTES), which provide amino groups, by means of which the HPA could be chemically immobilized and subsequently reduce

[a] *Dr. O. H. P. Cuervo, Dr. H. A. Rojas, Dr. J. J. Martínez*
Escuela de Ciencias Químicas, Facultad de Ciencias. Universidad Pedagógica y Tecnológica de Colombia UPTC Avenida Central del Norte, Tunja, Boyacá, Colombia
E-mail: jose.martinez@uptc.edu.co

[b] *Dr. L. A. Santos, Dr. T. C. Ramalho*
Departamento de Química, Universidade Federal de Lavras, Campus Universitário, Lavras, MG, 37200-000, Brazil

[c] *Dr. G. P. Romanelli*
Centro de Investigación y Desarrollo en Ciencias Aplicadas "Dr. J.J. Ronco" (CINDECA), Departamento de Química, Facultad de Ciencias Exactas, UNLP-CCT-CONICET. Calles 47 N° 257, B1900 AJK, La Plata, Argentina

Supporting information for this article is available on the WWW under https://doi.org/10.1002/slct.201801051

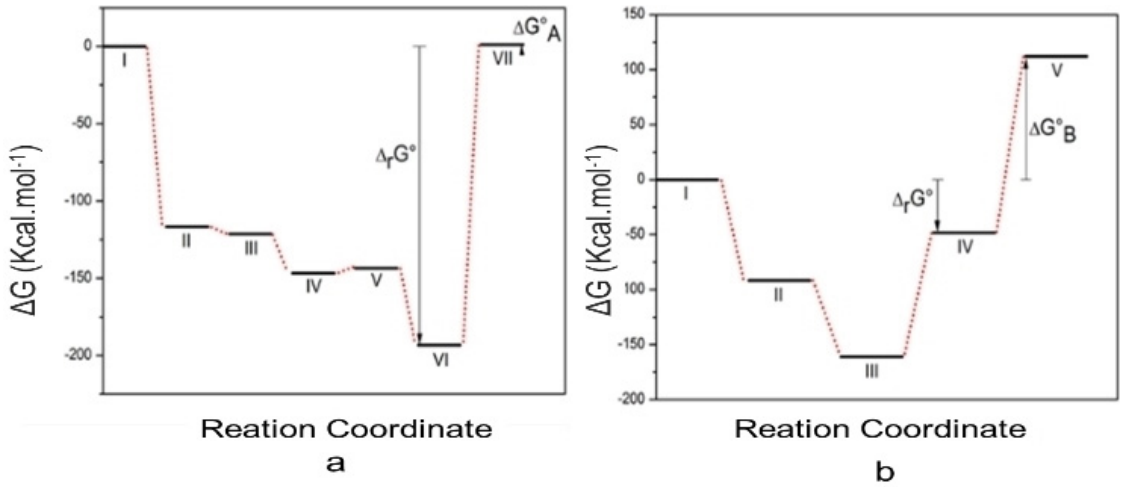

Figure 1. Gibbs energy in the mechanism proposed of HMF etherification (Figure 1a) and HMF oxidation (Figure 1b).

the leaching of the active sites.[12] However, although the introduction of APTMS on silica supports could effectively improve the stability of this type of catalyst during the reaction process, the HPA content is still far from sufficient for some specific reactions. This is probably because the number of silanol groups on the surface of the silica coating is limited and, consequently, the number of amino groups introduced by condensation between the silanol group and the amino-bearing organosilanes is restricted.[13] As a result, a support with sufficient anchor points is of great importance for having a high load of HPA with excellent durability. Consequently, cross-linking agents such as chitosan[14] and polyethyleneimine (PEI)[15] with abundant amino terminal groups have been used as a constituent of the shell to manufacture magnetic materials based on HPAs.

On the other hand, magnetic particles have been shown to be promising supports for the immobilization of catalysts because they can readily be separated from the reaction medium using an external magnetic field, which provides easy separation of the catalyst without having to filter, centrifuge or use other more cumbersome forms of separation.[16] In addition to an easy separation, another interesting property of the magnetic particles is that an appropriate surface modification provides a wide range of magnetically functionalized catalysts that exhibit an equal and sometimes greater activity than their homogeneous catalysts in organic transformations.[17]

Taking into account previous results, in this work a systematic study was performed using magnetic composites in which HPA-Preyssler was successfully immobilized onto the surface of PEI coating on magnetic Fe_3O_4 cores by chemical bonding between amino groups and HPA-Preyssler. To understand how the preferential formation of OBMF occurs, a thermodynamic study was performed.

Results and Discussion

Bulk HPA-Preyssler leads to the formation of OBMF as the main product (S_{OBMF} = 92%) and DFF (S_{DFF} = 8%) in lower proportion. The formation of OBMF is due to the self-etherification of HMF, while the formation of 2,5-diformyfuran (DFF) is the product of HMF oxidation. The preferential formation of OBMF depends on the acidity of the catalyst, while the formation of DFF is favored when HMF interacts with the W–O bond by hydrogen bonding. A thermodynamic study about the stability of the intermediates was performed to explain the formation of OBMF and DFF.

In points I and II the free reactants and HMF interact with the protonated HPA, respectively. In this case, the mechanism of self-etherification of 5-HMF, proposed by Musau and Munavu[4] based on the mechanism of Gillis and Beck,[18] involves the protonation of the hydroxyl group by the protons of the heteropolyacid (point III, Figure 1a).

This protonated hydroxyl group promotes another 5-HMF molecule by nucleophilic bimolecular substitution (SN_2) (point IV) followed by the formation of the H_3O^+ ion (point V). In stage VI the release of water occurs by the liberation of a proton to the HPA in order to restore the catalyst and generate OBMF as the main product. The Gibbs free energy of reaction (Δ_rG°) related from stages I to VI is -193.31 kcal.mol^{-1}. The final stage (VII) is the decomplexation of OBMF and H_2O molecules from the HPA with Gibbs free energy (ΔG°_A) of 1.14 kcal.mol^{-1}. Figure 2 shows the structures in each stage as a function of the proposed mechanism in the HMF etherification (Figure 1a).

Inspired by K. Ren et al.,[19] work, we propose an oxidation mechanism of HMF for obtaining DFF using HPA-Preyssler. The thermodynamics of this process is shown in Figure 1b. Stage I is the point in which the reactants are free, and the oxidation starts at point II, where 5-HMF interacts with the W–O by hydrogen connection bonding. Now, 5-HMF is the proton donor. Point III results from the transfer of protons from 5-HMF to oxygen bound to W. Then the W of the HPA-Preyssler binds to 5-HMF. In the last stage (IV), the heteropolyacid captures a

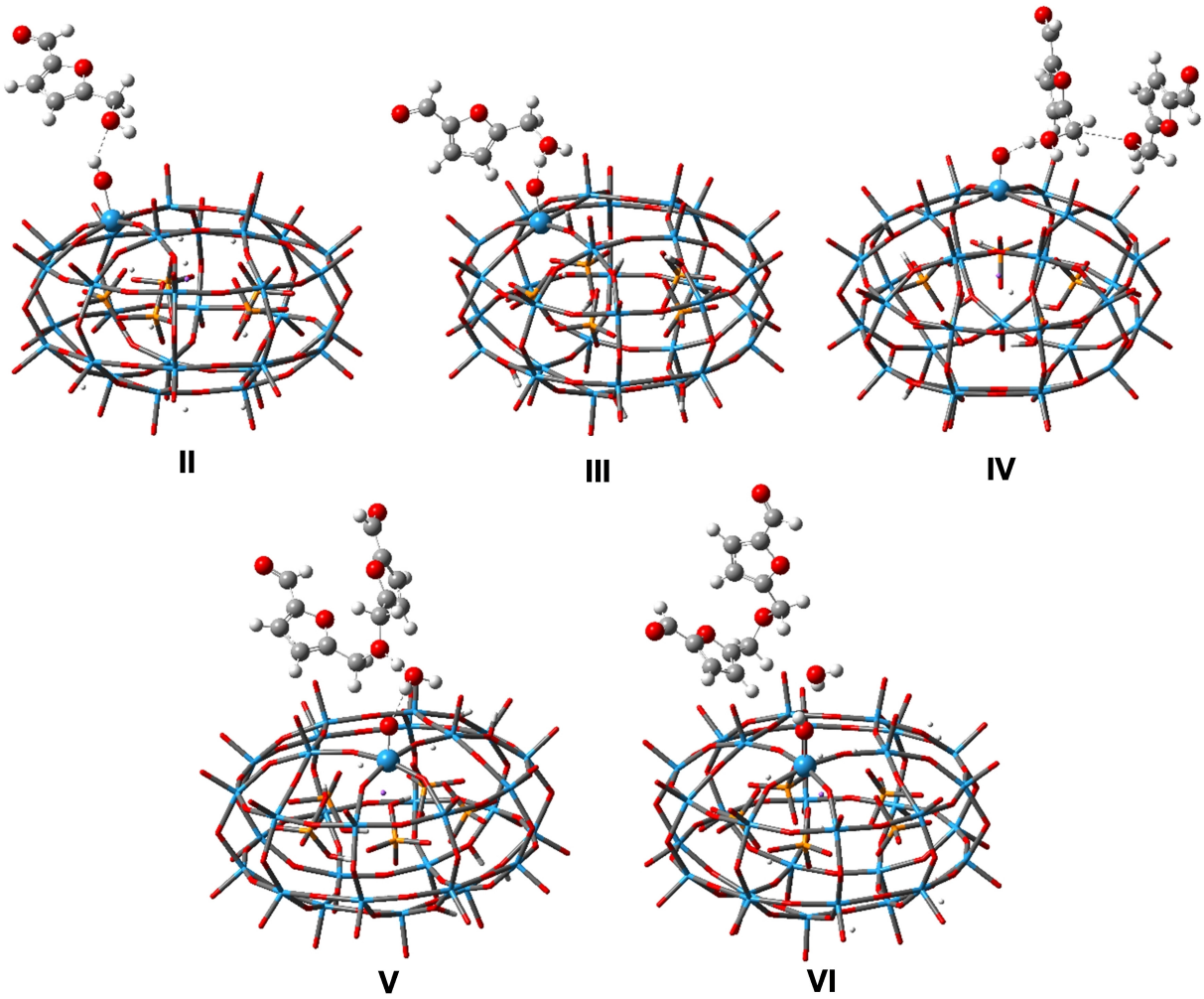

Figure 2. Structures of points II, III, IV, V and VI in Figure 1 Structures of points II, III and IV in Figure 1 FTIR spectra of pyridine adsorbed on (a) P/Al_2O_2 (b) P/SiO_2-Fe_3O_4 (c) P/SiO_2 (d) HPA-Preyssler. P = HPA-Preyssler, B = Brönsted acid sites, L = Lewis acid sites.

hydrogen bound to the nearest carbon, resulting in the oxidation of HMF to DFF. The Gibbs free energy of reaction ($\Delta_r G^\circ$) related from stage I to IV is −48.20 kcal.mol^{-1}. Point V is where the DFF comes off the catalyst, now with two more hydrogens. The Gibbs standard free energy with the decomplexation (ΔG°_B) is 112.11 kcal.mol^{-1}. Figure 3 shows the illustration of chemical species and points II, III and IV corresponding to the mechanism thermodynamically quantified in Figure 1b.

The competition between the etherification and oxidation of HMF is related to the interaction of protons that favors the formation of OBMF or the interaction with the W–O bond. The dispersion of HPA-Preyssler in supports with distinct characteristics decreases the conversion but favors a route of reaction depending on the charge distribution of the supported heteropolyacid. The results obtained for HPA/SiO_2, HPA/Al_2O_3 and P/SiO_2-Fe_3O_4 are listed in Table 1, and Figure 4 shows the FTIR spectra of pyridine adsorbed on those same materials. Also, for comparison, the nature of acid sites of the HPA-Preyssler sample are also displayed, which are in agreement with a previous report.[11] Although in supported heteropolyacids the conversion to OBMF decreases compared with the bulk, the selectivity depends on the support used (see entries 2 and 3).

Table 1. Activity results at 2 h of reaction of etherification of 5-HMF using supported HPA-Preyssler.

Entry	Catalyst*	α, (%)	S_{OBMF} (%)	S_{DFF} (%)	S_{Others} (%)	Y_{OBMF} (%)	Y_{DFF} (%)
1	P	85	92	8	0	78	7
2	P/SiO_2[a]	79	97	3	0	76	2
3	P/Al_2O_3[a]	9	43	57	0	4	5
4	P/SiO_2-Fe_3O_4[a]	76	68	13	11	52	10
5	P/SiO_2-Fe_3O_4[a] reuse	18	91	8	1	16	1.4

* Reaction conditions: 30 mg catalyst, [a] (23 wt% P), 0.26 mmol of 5-HMF, 343 K, 2 h of reaction, 2 mL of dichloromethane. α: conversion; S_{OMBF}: selectivity to OMBF; S_{DFF}: selectivity to DFF; S_{others} = selectivity to other compounds. P = HPA-Preyssler

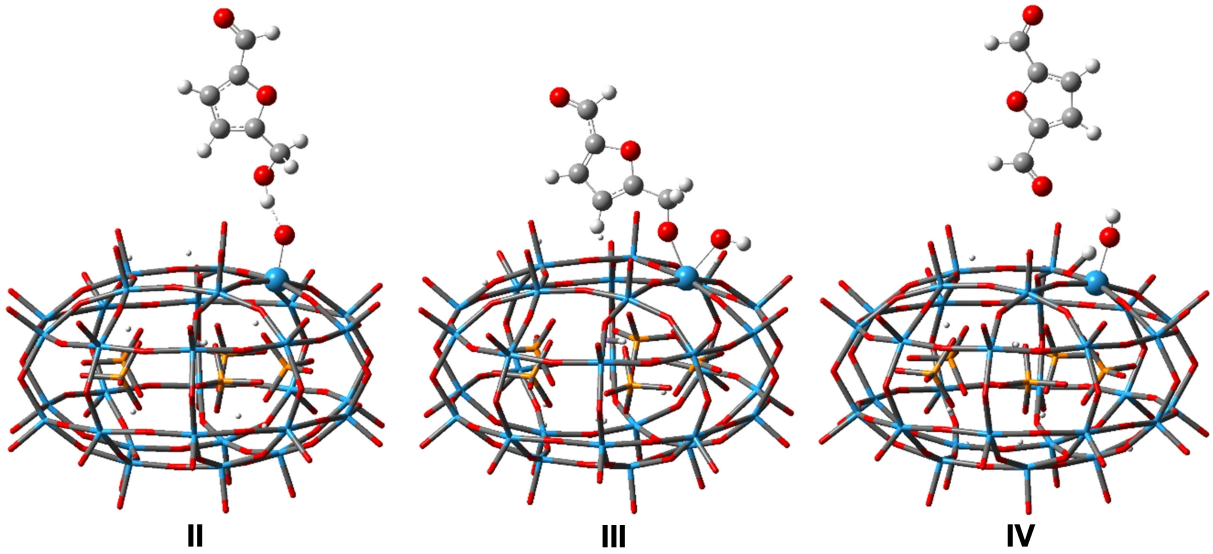

Figure 3. Structures of points II, III and IV in Figure 1b in light of the theoretical calculations for obtaining DFF. C atoms in grizzly balls, H atoms in white, O atoms in red, P atoms in orange, W atoms in blue and Na atoms in purple.

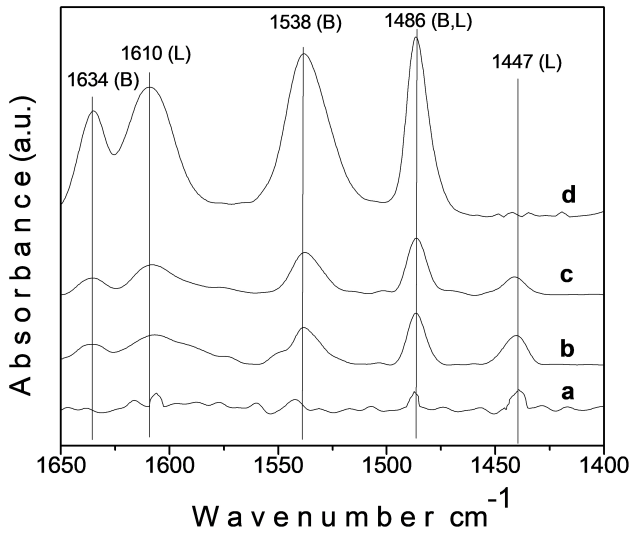

Figure 4. FTIR spectra of pyridine adsorbed on (a) P/Al_2O_2 (b) P/SiO_2-Fe_3O_4 (c) P/SiO_2 (d) HPA-Preyssler. P = HPA-Preyssler, B = Brönsted acid sites, L = Lewis acid sites.

The HPA-Preyssler supported on SiO_2 maintains the high selectivity to OBMF, due to the number and availability of Brönsted acid sites (Figure 4c). In HPA-Preyssler supported on Al_2O_3 the formation of DFF is a consequence of the lowest acidity (Figure 4a) that a negative charge typically possesses.[11] The availability of protons seems to be favored when HPA is supported on SiO_2 and leads to the formation of OBMF, while an excess of negative charge favors the electrostatic interaction of the HPA with -OH surface groups of the support and decreases proton availability leading to the formation of DFF.

Although the Preyssler/SiO_2 solid allows obtaining OBMF with good results, the reusability of this supported catalyst was not studied due to the difficulty of separating it from the reaction medium. The possibility of incorporating magnetic characteristics was also studied with the aim of achieving an easy separation from the reaction medium. It can be seen in entry 4 that the conversion of Preyssler/SiO_2-Fe_3O_4 was similar to that of Preyssler/SiO_2, which agrees with the number and availability of Brönsted acid sites (Figure 4b), but other products as well as DFF formed, possibly due to incomplete coverage of the magnetic particles that can act as oxidation catalysts. Although the separation of this solid is possible, a strong drop of the conversion was observed in the first reuse (entry 5), i.e., the HPA leached into the reaction medium (see Supporting Information, Table S1, entry 1) and consequently the conversion decreased. According to the results obtained, the percentage of leaching was determined by UV spectroscopy at 204 nm using a calibration curve (see Supporting Information, Figure S1).

In order to favor the formation of OBMF and avoid the formation of DFF, the HPA should have a high availability of protons. It can be observed that the selectivity depends on the support used, the separation and leaching of the HPA being the key problem. Thus, we decided to incorporate the HPA-Preyssler in a matrix that would allow the total coating of the magnetite and prevent the formation of DFF and by-products due to the presence of oxides that can act as oxidation catalysts.

The use of magnetic composites has been previously studied by our research group, demonstrating that the iron oxide particles can be completely coated in the cross-linking process with glutaraldehyde and polyethyleneimine. This was demonstrated by XPS analysis, where the absence of the signal associated with Fe $2p_{3/2}$ and $2p_{1/2}$ suggests that the Fe_3O_4 particles were totally covered.[20]

The functionalization with APTES was used to obtain Fe_3O_4-NH_2, which was then cross-linked with glutaraldehyde and PEI. The abundant terminal amino groups in PEI not only act as basic functional groups for anchoring the HPA-Preyssler, but also as nucleophilic functional groups that attack the carbon of glutaraldehyde to build a stable network on the surface of the magnetic core.[21] In order to determine the effect of glutaraldehyde on HPA-Preyssler anchoring and a stable network formation, two magnetic composites were synthesized. In the first, glutaraldehyde was added to the previously functionalized support and then PEI was added to increase the density of amino groups before immobilizing the HPA-Preyssler (Fe_3O_4-A–G-PEI–P). In the second magnetic composite, an extra amount of glutaraldehyde was added as a cross-linking agent after immobilizing the HPA-Preyssler (Fe_3O_4-A–G-PEI–P-G) to avoid the leaching of HPA. Where: A = APTES, G = Glutaraldehyde. Twenty-three percent of HPA was used for immobilization on the composite structures.

Table 2 displays the results of HMF etherification using the magnetic composites. The immobilization of HPA-Preyssler in Fe_3O_4 functionalized with APTES is very much lower, possibly because the amino groups on the magnetite surface neutralize the HPA protons. In addition, the large molecular size of HPA-Preyssler can prevent the anchoring of many molecules on the magnetite surface, which is reflected in the low conversion of HMF (entry 1) and was further confirmed by EDS analysis. When the density of amino groups is increased by reacting the amino groups from APTES with glutaraldehyde and PEI, the conversion is considerably higher (entry 2) because of the greater amount of immobilized HPA-Preyssler. However, when the reuse of this catalyst was tested (entry 3), the conversion decreased by 35% due to the leaching of HPA-Preyssler (see Supporting information, Table S1, entry 2). On the other hand, when glutaraldehyde was added as a cross-linking agent after immobilizing the HPA-Preyssler, the conversion decreased (entry 4). However, when testing the reuse of these solids, less HPA was lost in the cross-linked solid, decreasing the conversion by only 18% (entry 5) possibly due to poisoning of the catalyst, since no leaching was observed (see Supporting information, Table S1, entry 3).

Table 2. Activity results at 2 h of reaction the etherification reaction of 5-HMF using HPA-Preyssler immobilized on magnetic composites.

Entry	Catalyst	α (%)	S_{OBMF} (%)	S_{DFF} (%)	S_{Others} (%)	Y_{OBMF} (%)
1	Fe_3O_4-A-P	1.2	100	0	0	1.2
2	Fe_3O_4-A–G-PEI-P	62	100	0	0	62
3	Fe_3O_4-A–G-PEI–P (reuse)	40	93	6		37
4	Fe_3O_4-A–G-PEI–P-G	43	100	0	0	43
5	Fe_3O_4-A–G-PEI–P-G (reuse)	35	97	2.2	0	34

*Reaction conditions: 30 mg catalyst, (23 wt% P), 0.26 mmol of 5-HMF, 343 K, 2 h of reaction, 2 mL of dichloromethane. α: conversion; S_{OMBF}: selectivity to OMBF; S_{DFF}: selectivity to DFF; S_{Others}: Selectivity to other compounds. A = APTES, G = glutaraldehyde, PEI = polyethyleneimine, P = HPA-Preyssler.

To explain the catalytic behavior of the magnetic composites, some FTIR tests were performed. Figure 5 shows the FTIR

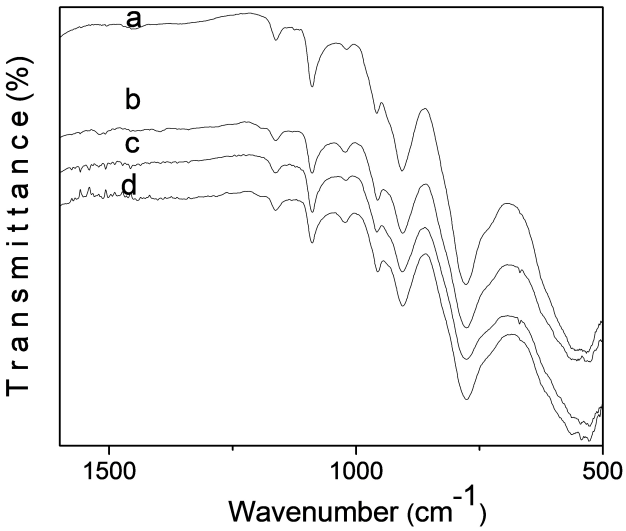

Figure 5. FTIR spectra of (a) Fe_3O_4-A–G-PEI–P, (b) Fe_3O_4-A–G-PEI–P (first reuse), (c) Fe_3O_4-A–G-PEI–P-G, (d) Fe_3O_4-A–G-PEI–P-G (first reuse).

of the composites obtained before and after the reaction. Two main findings can be observed; the intensity of the characteristic peaks of the HPA-Preyssler is higher in the solid Fe_3O_4-A–G-PEI–P (Figure 5a), but the intensity of these bands decreases considerably in this same solid after its first reuse (see bands at 1165, 1088, 1025 cm^{-1} associated with P–O bonds, and the bands at 957 and 901 cm^{-1} associated with stretching vibrations of W–O-W bonds)[22] (Figure 5b). Indeed, the composite without a new recovery of glutaraldehyde as a cross-linking agent does not favor the retention of HPA and consequently decreases its catalytic performance during reuses.

The bands around 1610 and 1447 cm^{-1} are assigned to pyridine adsorbed on Lewis acid sites, whereas the band around 1486 cm^{-1} is assigned to the interaction of pyridine on Brönsted and Lewis acid sites, and the bands at 1634 and 1538 cm^{-1} are ascribed to Brönsted acid sites[23] (see Supporting Information, Figure S2). In Fe_3O_4-A–G-PEI–P the intensity of the peaks corresponding to Brönsted acid sites is slightly similar to that of Fe_3O_4-A–G-PEI–P-G, which indicates that probably the recovery of the HPA by glutaraldehyde does not affect proton availability. However, in both cases the intensity of these bands is affected drastically with the first reuse, this change being higher in the solid where glutaraldehyde is not added to the composite after immobilization of the HPA-Preyssler. These results can be easily observed by quantifying the areas of the FTIR spectroscopy of pyridine adsorption (Table 3). Thus, glutaraldehyde effectively reacts with nearby amino groups forming a network that decreases the leaching of immobilized HPA-Preyssler when the composite is reused.

Table 3. Integration of the different bands shown in the Py-FTIR of the fresh and used catalysts (1 time/first reuse).

Catalyst	Total area	B (%)	L (%)	L–B (%)
Fe_3O_4-A–G-PEI-P	0.101	36	28	37
Fe_3O_4-A–G-PEI–P (first reuse)	0.042	38	29	33
Fe_3O_4-A–G-PEI–P-G	0.103	32	33	35
Fe_3O_4-A–G-PEI–P-G (first reuse)	0.051	40	26	34

B: Brönsted acid sites; L: Lewis acid sites; L–B: Brönsted-Lewis acid sites

The easy separation of magnetic composites is due to the magnetic behavior, which was tested by vibrating sample magnetometry (VSM) and compared with the behavior of Fe_3O_4 and Fe_3O_4-A. The hysteresis curves are shown in Figure 6. Little

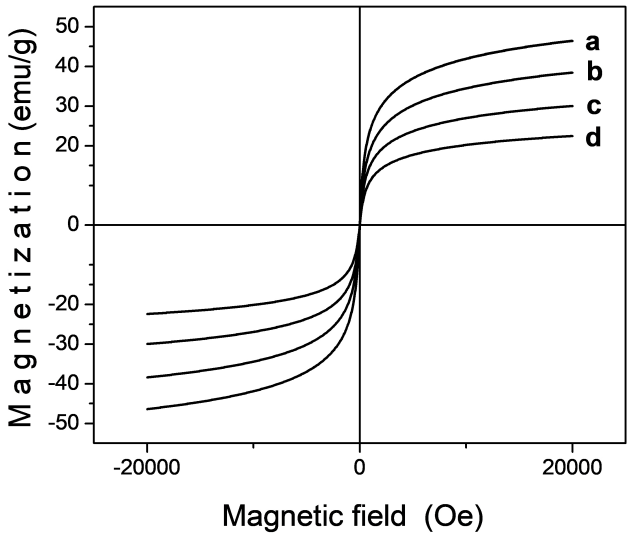

Figure 6. Magnetization hysteresis loops (298 K) of (a) Fe_3O_4, (b) Fe_3O_4-APTES, (c) Fe_3O_4-A–G-PEI–G, (d) Fe_3O_4-A–G-PEI–P-G

remanence or magnetic coercivity was observed in the samples, typical of a superparamagnetic behavior, and therefore, they can be easily dispersed when the applied magnetic field is withdrawn.[24]

The saturation magnetization (MS/Ms) values of the four samples are 46.3, 38.2, 29.7 and 22.3 emu/g for Fe_3O_4, Fe_3O_4-APTES, Fe_3O_4-A–G-PEI–P and Fe_3O_4-A–G-PEI–P-G, respectively. The distinct decrease in magnetization by mass saturation can be attributed to the gradual increase in the proportion of components without magnetic storages such as APTES, PEI and HPA-Preyssler:[14,25,15] However, solids can easily be removed from the reaction medium when an external magnetic field is applied as shown in Figure 7.

In order to evaluate the mass effects, the reaction of HMF to OBMF was conducted with Fe_3O_4-A–G-PEI–P-G. Figure 8a shows a typical behavior, where a higher mass causes an increase in the OBMF yield. It is interesting to note that by varying the mass of catalyst, OBMF formation does not favor

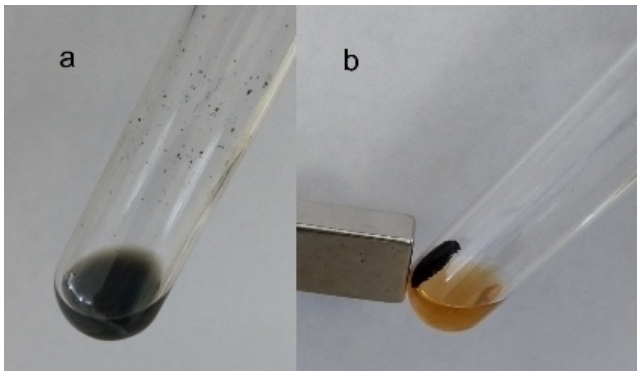

Figure 7. Easy recovery of Fe_3O_4-A–G-PEI–P-G. (a) Appearance at the end of etherification reaction. (b) Separation of the magnetic composite with a magnet.

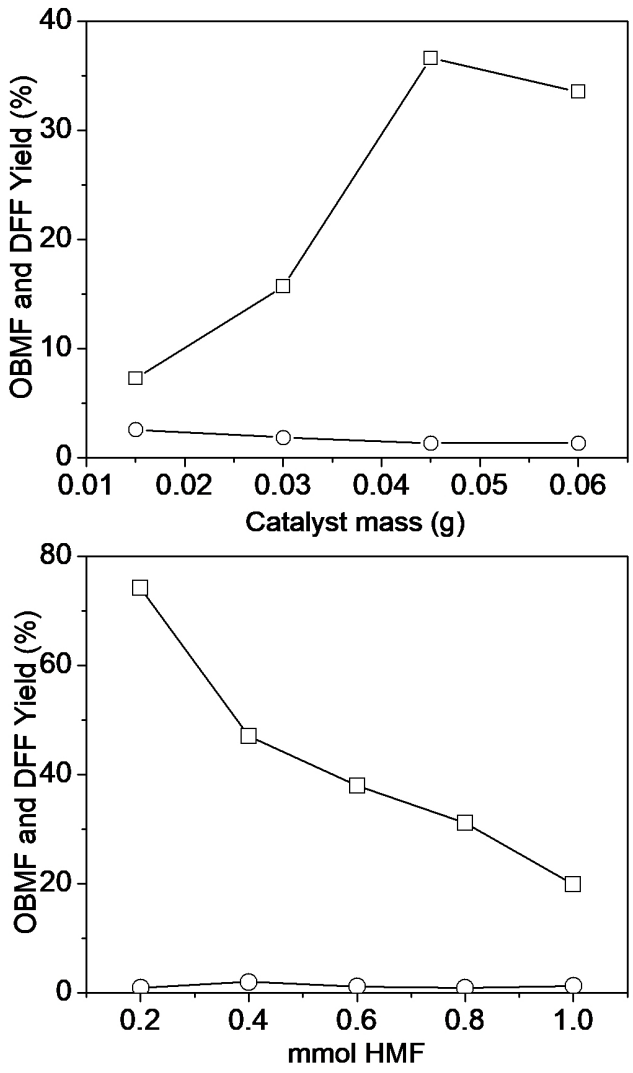

Figure 8. Catalyst mass effect (343 K, 0.26 mmol HMF). Effect of the amount of HMF (mmol) (343 K, 45 mg catalyst). ○ = yield to DFF; □ = yield to OBMF

the formation of DFF, as a consequence of a higher number of acid sites. However, OBMF decreased when using a high catalyst mass without affecting the DDF yield probably due to diffusional problems. The amount of HMF was also studied (Figure 8b) demonstrating that it decreased with a higher amount of HMF because of saturation in the active sites of HPA-Preyssler.

Finally, using 45 mg of catalysts, and 0.2 mmol HMF, the catalyst recycling of the magnetic composite was studied in 5 consecutive reactions. Before each reaction, the catalyst was separated by an external magnet, washed with dichloromethane (3x3 mL) and dried. The FTIR spectrum of the recycled catalyst shows no change after 5 successive cycles and that the typical peaks of the HPA structure remained. The percentage yields and the selectivity of each recycle are shown schematically in Figure 9, which indicates only a modest decrease in

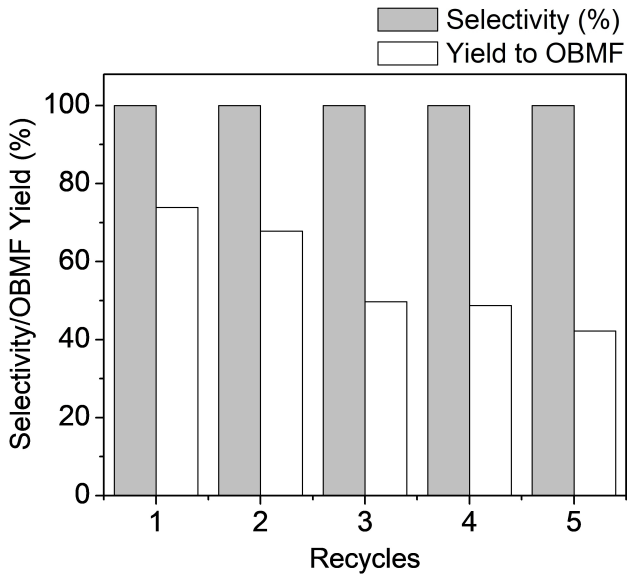

Figure 9. Recycling of Fe_3O_4-A–G-PEI–P-G: Catalyst, 45 mg, 0.2 mmol of 5-HMF, 343 K, 0.5 mL CH_2Cl_2 and 5 h of reaction.

catalytic performance after the first run. Subsequently, in the next 3 runs the yield decreased a little more due to the adsorption of reagents and products on the catalyst surface, which may be associated with the decrease in the intensity of the characteristic peaks of HPA-Preyssler and the appearance of new bands in the FTIR of the catalyst used for 5 consecutive cycles (see Supporting Information, Figure. S3) and not to the leaching of HPA-Preyssler. For this reason, the selectivity remained constant during the reuse tests, which reveals a satisfactory reusability of Fe_3O_4-A–G-PEI–P-G.

Conclusions

The competition between the etherification and oxidation of HMF using HPA-Preyssler is related to the interaction of protons that favors the formation of OBMF or the interaction with the W–O bond. The dispersion of HPA-Preyssler in metallic oxides does not favor the formation of OBMF and reduces the reusability; however, in magnetic composites proton availability is favored and consequently, the formation of OBMF is preferentially obtained. To avoid the leaching of heteropolyacid a new recovery with glutaraldehyde was necessary. The easy separation of magnetic composites is due to the magnetic behavior, which is preserved in the composites obtained. A percentage yield of 73.1% was obtained with 0.2 mmol of HMF, 45 mg of magnetic composite and 343 K at 5 h of reaction, which decreased slightly in 5 consecutive cycles. However, the selectivity remained constant during the reuse tests.

Supporting information summary

Experimental section, the percentage HPA-Preyssler leached from magnetic composites, UV-vis spectra of HPA-Preyssler and results of some characterization of the catalysts, after some reuse are described in the Supporting Information.

Acknowledgements

We thank COLCIENCIAS for the financial support under project No. 110965843004. GPR thanks CONICET, UNLP, MINCYT and the European Research Area Network, ERANet LAC (ref. ELAC2014/BEE-0341). The authors thank Carlos A.M. Afonso for the contributions to this manuscript. Dr. Afonso is the leader of ERANet LAC project.

Conflict of Interest

The authors declare no conflict of interest.

Keywords: magnetic composites · preyssler heteropolyacid · reusability · thermodynamic study

[1] R. Van Putten, J. C. Van Der Waal, E. De Jong, C. B. Rasrendra, H. J. Heeres, J. G. De Vries, *Chem. Rev.* **2013**, *113*, 1499–1597.
[2] C. Moreau, M. Naceur, A. Gandini, *Top. Catal.* **2004**, *27*, 11–30.
[3] L. R. Wen, F. Yu, X. Dong, Miao Y., P. Zhou, Z. Lin, J. Zheng, H. Wang, D. Q. Huang, CN 1456556. **2003**.
[4] R. M. Musau R. M. Munavu, *Biomass* **1987**, *13*, 67–74.
[5] E. R. Sacia, M. Balakrishnan, A. T. Bell, *J. Catal.* **2014**, *313*, 70–79.
[6] W. Fang, et al., *Catal. Sc.Technol.* **2015**, *5*, 3980–3990.
[7] O. Casanova, S. Iborra, A. Corma, *J. Catal.* **2010**, *275*, 236–242.
[8] H. Wang, Y. Wang, T. Deng, G. Chen, Y. Zhu, X. Hou, *Catal. Commun.* **2015**, 59, 127–130.
[9] K. Mliki, M. Trabelsi, *Ind. Crops Prod.* **2015**, *78*, 91–94.
[10] S. Shinde, C. Rode, *Catal. Commun.* **2017**, *88*, 77–80.
[11] A. Paez, H. A. Rojas, O. Portilla, C. A. M. Afonso, G. P. Romanelli, J. J. Martínez, *ChemCatChem* **2017**, *9*, 3322–3329.
[12] M. Gil, I. Tiscornia, Ó. De, R. Mallada, J. Santamaría, *Chem. Eng. J.* **2011**, *175*, 291–297.
[13] I. V Kozhevnikov, *Chem. Rev.* **1998**, *98*, 171–198.
[14] S. Li, S. R. Zhai, J. M. Zhang, Z. Y. Xiao, Q. Da An, M. H. Li, X. W. Song, *Eur. J. Inorg. Chem.* **2013**, *31*, 5428–5435.
[15] Z. Zhang, F. Zhang, Q. Zhu, W. Zhao, B. Ma, Y. Ding, *J. Colloid Interface Sci.* **2011**, *360*, 189–194.
[16] V. Polshettiwar, R. Luque, A. Fihri, H. Zhu, M. Bouhrara, J. M. Basset, *Chem. Rev.* **2011**, *111*, 3036–3075.

[17] H. Eshghi, A. Javid, A. Khojastehnezhad, F. Moeinpour, F. F. Bamoharram, M. Bakavoli, M. Mirzaei, *Chinese J. Catal* **2015**, *36*, 299–307.
[18] B. T. Gillis, P. E. Beck, *Org. Chem* **1963**, *28*, 1388–1390.
[19] K. Ren, H.-Q. Yang, C.-W. Hu, *Catal. Sci. Technol.* **2016**, *6*, 3776–3787.
[20] A. Y. Vargas, H. A. Rojas, G. P. Romanelli, J. J. Martínez, *Green Process. Synth.* **2017**, *6*, 377–384.
[21] I. Creaser, M. C. Heckel, R. J. Neitz, M. T. Pope, *Inorg. Chem.* **1993**, *32*, 1573–1578.
[22] B. Luo, X. J. Song, F. Zhang, A. Xia, W. L. Yang, J. H. Hu, C. C. Wang, *Langmuir* **2010**, *26*, 1674–1679.
[23] R. Ferwerda, J. H. van der Maas, F. B. van Duijneveldt, *J. Mol. Catal. A Chem.* **1996**, *104*, 319–328.
[24] J. Sun, G. Yu, L. Liu, Z. Li, Q. Kan, Q. Huo, J. Guan, Catal. *Sci. Technol.* **2014**, *4*, 1246–1252.
[25] F. Hosseini, M. Seyedsadjadi, N. Farhadyar, *Orient. J. Chem.* **2014**, *30*, 4, 1609–1618

Submitted: April 10, 2018
Revised: May 4, 2018
Accepted: May 11, 2018